AAS 15-663

ANALYTIC POWER SERIES SOLUTIONS FOR TWO-BODY AND J_2–J_6 TRAJECTORIES AND STATE TRANSITION MODELS

Kevin Hernandez[*], Julie L. Read[*], Tarek A. Elgohary[†], James D. Turner[‡], and John L. Junkins[§]

Recent work has shown that two-body motion can be analytically modeled using analytic continuation models, which utilize kinematic transformation scalar variables that can be differentiated to an arbitrary order using the well-known Leibniz product rule. This method allows for large integration step sizes while still maintaining high accuracy. With these arbitrary order time derivatives available, an analytical Taylor series based solution may be applied to propagate the position and velocity vectors for the nonlinear two-body problem. This foundational method has been extended to demonstrate a highly effective variable step-size control for the analytic continuation Taylor series model. The current work builds on these earlier results by extending the analytic power series approach to trajectory calculations for two-body and J_2–J_6 gravity perturbation terms.

INTRODUCTION

From Newtonian mechanics, the dynamics of the relative motion for the perturbed two-body problem is given by,

$$\ddot{\mathbf{r}} = -\frac{\mu}{r^3}\mathbf{r} + \mathbf{a}_d \tag{1}$$

where, $\mathbf{r} = [x, y, z]^{\mathrm{T}}$ is the inertial relative position, $\mu = G(m_1 + m_2)$ the gravitational mass parameter, $r = \sqrt{\mathbf{r} \cdot \mathbf{r}}$ and $\mathbf{a}_d$ refers to the perturbation acceleration. For the unperturbed/classical two-body problem, $\mathbf{a}_d = \mathbf{0}$, Eq. (1) has an analytical solution extracted from the conservation of angular momentum and the fundamental orbit integrals.[1,2] The Lagrange/Gibbs,"*F&G*", solution expresses the future state vector as a projection onto the initial position and velocity, where F and G are themselves nonlinear function of the initial state.[1,2] The recursion of the equation produced by successive differentiation has also been exploited to produce a power series based solution with Lagrange Fundamental Invariants.[1]

For the general two-body problem, where $\mathbf{a}_d \neq 0$, several numerical techniques exist to handle the solution of the nonlinear initial value problem (IVP) in Eq. (1). The Runge-Kutta, *RK*, family of methods can be considered as the most widely used explicit methods for numerical integration.

[*]Graduate Research Assistant, Department of Aerospace Engineering, Texas A&M University, H.R. Bright Bldg, 3141 TAMU, College Station, TX 77843-3141

[†]Postdoctoral Research Associate, Department of Aerospace Engineering, Texas A&M University, H.R. Bright Bldg, 3141 TAMU, College Station, TX 77843-3141

[‡]TEES Research Professor, Department of Aerospace Engineering, Texas A&M University, H.R. Bright Bldg, 3141 TAMU, College Station, TX 77843-3141

[§]Distinguished Professor, Department of Aerospace Engineering, Texas A&M University, H.R. Bright Bldg, 3141 TAMU, College Station, TX 77843-3141

Adaptive step-size 4th-order *RK* methods have been developed and are known as the Runge-Kutta-Fehlberg, *RKF*, methods.[3] Higher order adaptive *RK* methods have also been developed for high accuracy requirement applications. Adaptive Runge-Kutta-Nyström, *RKN*, methods with order 8(7), 9(8), 10(9) and 11(10) have been used to solve general second-order ordinary differential equations.[4] For orbit propagation problems, the Gauss-Jackson method was studied extensively and compared against other numerical techniques, e.g. *RK4*, *RKN* and analytical continuation based Taylor series expansion.[5] It is a predictor-corrector finite difference method designed specifically for solving second order differential equations.[6,7] The *RKN12(10)* and *RKN8(6)* methods were introduced for general dynamical systems.[8] The methods were then compared against several Nyström methods and recursive power series solutions for orbit propagation problems.[9,10] Furthermore, the accuracy of several of the above mentioned numerical integrators are tested in solving different N-body problems such as, Sun, Jupiter, Saturn, Uranus, and Neptune and nine planet problems.[11] Most of the comparisons performed in the literature address the issue of tuning the integration step-size where the need for a high accuracy solution in many cases necessitates a small time-step.

Modified Chebyshev-Picard Iteration (*MCPI*) method has been developed for orbit propagation and general initial value problems.[12,13] The method combines orthogonal basis functions, Chebyshev polynomials, with Picard iterations to solve the initial value problem (IVP). It is used in long-term orbit propagation problems and shows improvement over the *RKN12(10)* in terms of computational cost.[12] Parallelization of *MCPI* is then explored and shows a substantial improvement in computational cost over Runge-Kutta single-step methods for several initial value problems including a near circular orbit for the classical two-body problem.[13] Since the initial introduction of *MCPI*, several contributions have been made to enhance the efficiency and the applicability of the method to a variety of astrodynamics problems. High order gravity perturbation models have been developed to capture motion of satellites near Earth.[14] Some of the enhancements that have been applied to *MCPI* include *MATLAB* libraries, variable fidelity and radially adaptive gravity approximations, segmentation/order tuning, multi-orbit accuracy and numerical stability studies, Kustaanheimo- Stiefel regularization and using the Method of Particular Solutions, *MMS*, to solve Two-Point Boundary Value Problems (TPBVPs) and Optimal Control Problems (OCPs).[15–22]

Furthermore, Implicit Runge-Kutta methods, *IRK*, have been explored for orbit propagation purposes.[23–25] The methods generally show very good convergence characteristics as well as computational efficiency comparable to the industry standard 8^{th} order Gauss-Jackson. Additionally, direct collocation techniques with Radial Basis Functions (RBFs) have been used to investigate general IVPs, Two Point Boundary Value Problems (TPBVPs), Optimal Control Problems (OCPs) and orbit propagation problems. Similar to *IRK* methods, the proposed methods show fast convergence and highly accurate results.[26–28]

Recent work by Turner and Elgohary has shown that Two-Body and J_2 gravity perturbation terms can be analytically modeled using Analytic Continuation (*AC*) methods.[29–33] They demonstrate that arbitrary order time derivatives for the trajectory motion can be generated by introducing three steps. First, nonlinear kinematic transformations are introduced for representing the vector behavior of the 3-D motion. Second, the two-body dynamics are transformed in terms of the new kinematic variables, and Leibniz product rule is invoked to generate arbitrary order time derivative models. Finally, a system-level recursive solution is achieved by linking the time derivative models for the newly defined nonlinear transformation variables with the equation of motion model. The resulting algorithm is fast, accurate, and simple to model. This work has been extended by Turner and Kim to demonstrate a highly effective variable step-size control for the analytic continuation Taylor series

model.[34]

The current work builds on these earlier results by extending the analytic power series approach to the trajectory calculations of the two-body as well as J_2–J_6 gravity perturbation terms. The algorithm is enhanced with a backward Horner summation and a variable time-step scheme, which enable convergence to machine precision and arbitrary order expansions of the series. These developments overcome some of the numerical limitations on power series approximations for the two-body problem and enable a fast, accurate and easy to implement solution algorithm. The basic trajectory generation capabilities are further extended for the calculation of state transition matrices. This is accomplished by partitioning the state transition matrix and evaluating the partitioned components for arbitrary order time derivatives by invoking Leibniz product rule. Numerical results from the series solution algorithm are introduced for three types of orbits for both the unperturbed and the perturbed dynamics. The analytic continuation algorithm achieves high convergence up to machine precision in conservation of total energy as well as in state error comparisons against *F&G* and *MCPI*.

ANALYTIC CONTINUATION METHOD

Two nonlinear kinematic transformation scalar variables serve to eliminate fraction terms typically found in arbitrary order time derivative models and are defined by,[29]

$$f = \mathbf{r} \cdot \mathbf{r} \tag{2}$$

$$g_p = f^{-p/2} \tag{3}$$

where $\mathbf{r}$ is the position vector and p denotes factors $3, 5, 7, 9, \ldots$ for the two-body, $p = 3$, and gravity correction terms, $p = 5, 7, 9, \ldots$. Here, f is a quadratic measure of distance and g is a constraint equation based on f. Leibniz product rule is directly applied to f, where the product is the vector dot product, and the n^{th} order time derivative of f is computed as the dot product:

$$f^{(n)} = \sum_{m=0}^{n} \binom{n}{m} \mathbf{r}^{(m)} \cdot \mathbf{r}^{(n-m)} \tag{4}$$

where $r^{(m)} = \frac{d^m r}{dt^m}$ and $\binom{n}{m} = \frac{n!}{m!(n-m)!}$ is the binomial coefficient. Note that all derivatives of $\mathbf{r}$ must be computed prior to invoking the above equation. The key step involves replacing the expression for g with a first-order differential equation, which is easily handled by applying Leibniz product rule to implement an implicit differential equation and consequently generate time derivatives of f and g:

$$f\dot{g}_p + \frac{p}{2} g_p \dot{f} = 0 \tag{5}$$

$$g_p^{(n+1)} = -\frac{1}{f}\left[\frac{p}{2} f^{(1)} g^{(n)} + \sum_{m=1}^{n} \binom{n}{m} \left(\frac{p}{2} f^{(m+1)} g^{(n-m)} + f^{(m)} g^{(n-m+1)}\right)\right] \tag{6}$$

Using these recursive solutions for f and g, we can recursively generate vector solutions for $\mathbf{r}^{(n)}$ to an arbitrary order. The perturbation term $\mathbf{a}_d$ in Eq. (1) can also be expressed in terms of the f and g scalars for J_2–J_6 zonal harmonics as:

$$\mathbf{a}_{J2} = -\frac{3}{2} J_2 \mu r_{eq}^2 \begin{Bmatrix} xg_5 - 5xz^2 g_7 \\ yg_5 - 5yz^2 g_7 \\ 3zg_5 - 5z^3 g_7 \end{Bmatrix} \tag{7}$$

$$\mathbf{a}_{J3} = \frac{1}{2} J_3 \mu r_{eq}^3 \begin{Bmatrix} 5\left(7xz^3 g_9 - 3xzg_7\right) \\ 5\left(7yz^3 g_9 - 3yzg_7\right) \\ 3\left(g_5 - 10z^2 g_7 + \frac{35}{3} z^4 g_9\right) \end{Bmatrix} \tag{8}$$

$$\mathbf{a}_{J4} = \frac{5}{8} J_4 \mu r_{eq}^4 \begin{Bmatrix} 3xg_7 - 42xz^2 g_9 + 63xz^4 g_{11} \\ 3yg_7 - 42yz^2 g_9 + 63yz^4 g_{11} \\ 15zg_7 - 70z^3 g_9 + 63z^5 g_{11} \end{Bmatrix} \tag{9}$$

$$\mathbf{a}_{J5} = \frac{1}{8} J_5 \mu r_{eq}^5 \begin{Bmatrix} 3\left(35xzg_9 - 210xz^3 g_{11} + 231xz^5 g_{13}\right) \\ 3\left(35yzg_9 - 210yz^3 g_{11} + 231yz^5 g_{13}\right) \\ 693z^6 g_{13} - 945z^4 g_{11} + 315z^2 g_9 - 15g_7 \end{Bmatrix} \tag{10}$$

$$\mathbf{a}_{J6} = -\frac{1}{16} J_6 \mu r_{eq}^6 \begin{Bmatrix} 35xg_9 - 945xz^2 g_{11} + 3465xz^4 g_{13} - 3003xz^6 g_{15} \\ 35yg_9 - 945yz^2 g_{11} + 3465yz^4 g_{13} - 3003yz^6 g_{15} \\ 245zg_9 - 2205z^3 g_{11} + 4851z^5 g_{13} - 3003z^7 g_{15} \end{Bmatrix} \tag{11}$$

where the values of the zonal harmonics, J_2–J_6 are given by:[2]

$$\begin{array}{lll} J_2 = 1082.63 \times 10^{-6} & J_3 = -2.52 \times 10^{-6} & J_4 = -1.61 \times 10^{-6} \\ J_5 = -0.15 \times 10^{-6} & J_6 = 0.57 \times 10^{-6} & \end{array} \tag{12}$$

and $\mu = 398600.4418\,\mathrm{km}^3\mathrm{s}^{-2}$ is the Earth gravitational parameter and $r_{eq} = 6378.1366 \times 10^3\,\mathrm{km}$ is the Earth equatorial radius.

The corresponding classical power series solution technique expresses the evolved trajectory solution as

$$\mathbf{r}(t+h) = \mathbf{r}(t) + \dot{\mathbf{r}}(t)h + \frac{\ddot{\mathbf{r}}(t)h^2}{2!} + \frac{\dddot{\mathbf{r}}(t)h^3}{3!} + \cdots \tag{13}$$

$$\mathbf{v}(t+h) = \dot{\mathbf{r}}(t) + \ddot{\mathbf{r}}(t)h + \frac{\dddot{\mathbf{r}}(t)h^2}{2!} + \frac{\mathbf{r}^{(4)}(t)h^3}{3!} + \cdots \tag{14}$$

where h represents the time-step chosen for propagating the dynamics. As with any power series-based approximation, the following issues must be addressed: (1) how many terms need to be retained in the approximations, (2) how large can the step-size h be made for maintaining a specified level of position and velocity accuracy, (3) can variable step-size algorithms be developed for accelerating the series approximations, and (4) what is the computational performance of the series approximation when compared to other available approximation methods. Early numerical results

obtained by summing the series from lowest-to-highest derivatives produce accurate and stable results depending on both the number of terms retained in the approximation and the size of the time propagation step, h. However, initial efforts to increase the time step leads to numerical stability issues.[29,31] To overcome this limitation the series solution is evaluated in reverse order using a Horner summation scheme, which effectively sums the smaller terms first and enables a more stable series solution at high orders. The reverse Horner scheme implemented in this work is shown in Algorithm 1.

Algorithm 1 Reverse Horner Scheme

```
procedure HORNER−SCHEME
    v1 = R(:,n-1) + (h/n)*R(:,n)        ▷ Initialize position vector summation
    v2 = R(:,n)                         ▷ Initialize velocity vector summation
    for i = n-1 → 1 do                  ▷ Loop for summing Taylor series terms
        T = h/i                         ▷ Time/factorial term ration
        v1 = R(:,i-1) + T*v1            ▷ sum i − 1 term for position
        v2 = R(:,i) + T*v2              ▷ sum i − 1 term for velocity
    end for
    xf = v1                             ▷ Update position vector
    vf = v2                             ▷ Update velocity vector
end procedure
```

In addition, Kim and Turner determine a variable step size scheme using the expression in Eq. (15) with increments that correspond to near-linear increments in true anomaly.[34]

$$h = \left(\frac{n!\, tol}{|\mathbf{r}^{(n)}|} \right)^{1/n} \tag{15}$$

where n denotes the order of the series expansion and tol defines the specified target tolerance. The generation of the variable time-step h from (15) is a key decision that governs efficiency and accuracy of the analytical continuation algorithm as will be shown.

Implementing all the above mentioned developments in the Analytic Continuation algorithm improves the stability and the adaptability of the method to handle a variety of orbit propagation IVPs as will be shown in the numerical results section. In addition, Leibniz rule as a fundamental concept combined with the Analytic Continuation algorithm has a clear impact on deriving the State Transition Matrix for various astrodynamics problems, as will be briefly shown below.

Development of the State Transition Matrix

State transition matrices (STMs) give us a measure of the uncertainty of the initial conditions and can be computed by utilizing the scalar transformation variables at each time step. STMs are used in many celestial mechanics optimization calculations, such as obtaining solutions for Lambert's problem. The series-based approach is extended to the state transition matrix calculation by the following steps. The first order differential equation for the state transition matrix is given by

$$\dot{\phi} = \nabla f \cdot \phi \tag{16}$$

This equation could be written using Leibniz's product rule as

$$\phi^{n+1} = \sum_{m=0}^{n} \binom{n}{m} \nabla f^n \phi^{n-m} \tag{17}$$

However, we can instead expand into partitions to obtain

$$\begin{bmatrix} \dot{\phi}_{11} & \dot{\phi}_{12} \\ \dot{\phi}_{21} & \dot{\phi}_{22} \end{bmatrix} = \begin{bmatrix} 0_{3x3} & I_{3x3} \\ G_{3x3} & 0_{3x3} \end{bmatrix} \begin{bmatrix} \phi_{11} & \phi_{12} \\ \phi_{21} & \phi_{22} \end{bmatrix} \tag{18}$$

Hence,

$$\dot{\phi}_{11} = \phi_{21} \tag{19}$$

$$\dot{\phi}_{12} = \phi_{22} \tag{20}$$

$$\dot{\phi}_{21} = G\phi_{11} \tag{21}$$

$$\dot{\phi}_{22} = G\phi_{12} \tag{22}$$

where G is the gradient of the two-body and higher-order gravity correction terms.[2] In this form, the Leibniz product rule applies as follows:

$$\phi_{11}^{(n+1)} = \phi_{21}^{(n)} \tag{23}$$

$$\phi_{12}^{(n+1)} = \phi_{22}^{(n)} \tag{24}$$

$$\phi_{21}^{(n+1)} = \sum_{m=0}^{n} \binom{n}{m} G^{(m)} \phi_{11}^{(n-m)} \tag{25}$$

$$\phi_{22}^{(n+1)} = \sum_{m=0}^{n} \binom{n}{m} G^{(m)} \phi_{12}^{(n-m)} \tag{26}$$

which are trivially incorporated into a power series solution algorithm with the initial conditions defined by the identity matrix, $\Phi(t_0, t_0) = I$. This power series, given below, is computed for each submatrix, and the final solution is then concatenated.

$$\phi(t+h) = \phi(t) + \dot{\phi}(t)h + \frac{\ddot{\phi}(t)h^2}{2!} + \frac{\dddot{\phi}(t)h^3}{3!} + \cdots \tag{27}$$

NUMERICAL SIMULATIONS RESULTS

The analytical continuation method is implemented for given initial position and velocity vectors, time interval, derivative expansion order, and optionally a list of time instants at which the solution must be computed (this enables comparing with other methods at the same nodes). The known position and velocity are computed, and the acceleration vector is evaluated. The first two derivatives of f and g are computed analytically, and then recursive loops compute the higher derivatives for f, g, and $\mathbf{r}$. This process is analytically continued for position and velocity using a power series expansion for all time steps until the final time is reached. Figure 1 gives an overview of the process.

Three different orbits were chosen to test the proposed method. For each case, both unperturbed and J_2-perturbed IVPs are numerically integrated with the Analytic Continuation, *AC*, algorithm. The three types of orbits selected are:

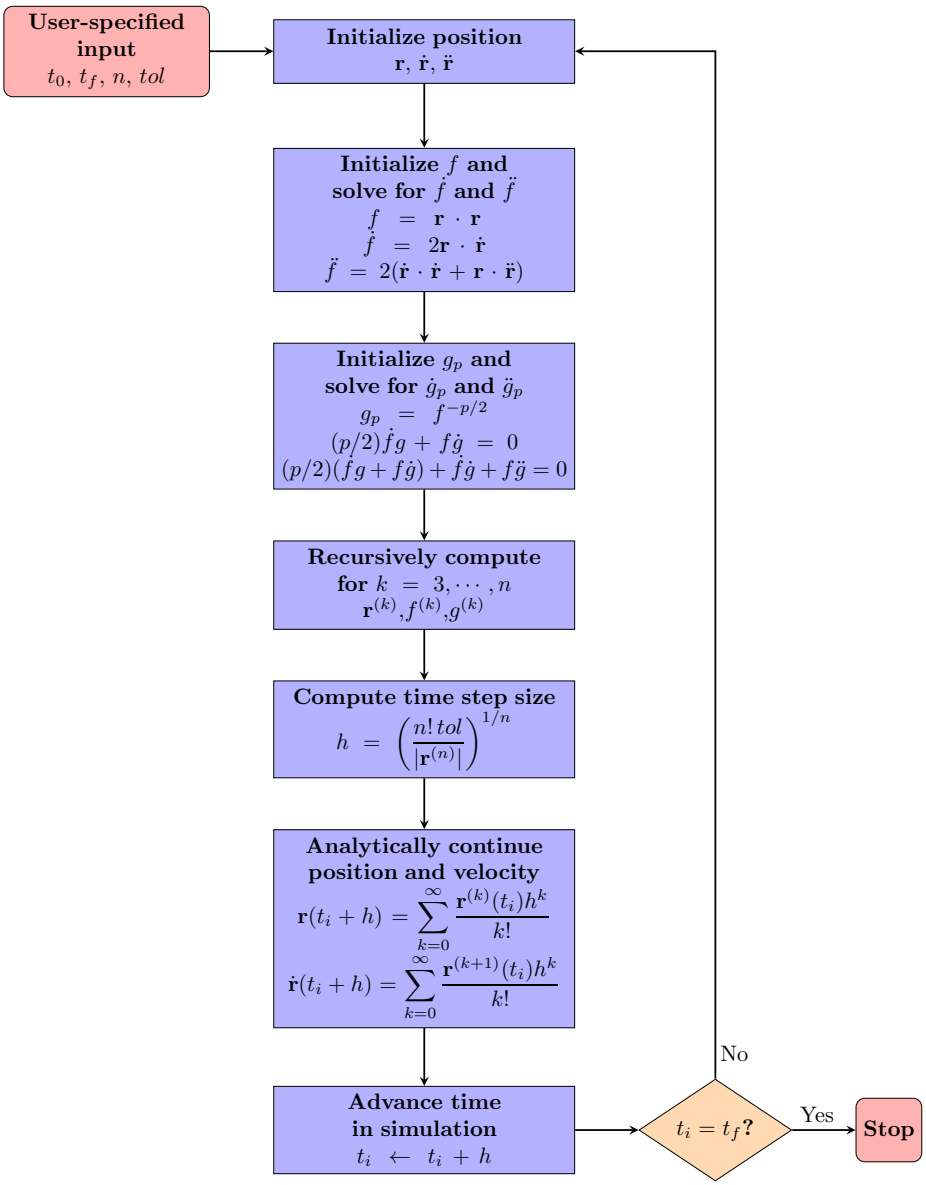

Figure 1. Flow Diagram for Analytical Continuation Solution Process

- A geostationary orbit (GEO) initialized with initial position $\mathbf{r}_0 = [4.224112, 0, 0]^T \times 10^7$ m and initial velocity $\mathbf{v}_0 = [0, 3.071858, 0]^T \times 10^3$ m/s; it has a semimajor axis $a = 4.224112 \times 10^7$ m and an eccentricity $e = 0$.
- An inclined, low earth orbit (LEO) initialized with initial position and initial velocity given by $\mathbf{r}_0 = [2.8654, 5.1911, 2.8484]^T \times 10^6$ m, and $\mathbf{v}_0 = [-5.3862, -0.3867, 6.1232]^T \times 10^3$ m/s, respectively; it has a semimajor axis $a = 8.439279069 \times 10^6$ m and an eccentricity $e = 0.672$.
- A highly elliptical orbit (HEO) initialized at its perigee with initial position $\mathbf{r}_0 = [7, 0, 0]^T \times 10^6$ m and initial velocity $\mathbf{v}_0 = [0, 1.0401526536, 0]^T \times 10^4$ m/s; it has a semimajor axis $a = 7.00025299 \times 10^7$ m and an eccentricity $e = 0.900$.

For each case, the integration time was set to the unperturbed period for the given initial conditions:

$$t_f = T = 2\pi \frac{a^{3/2}}{\sqrt{\mu}} \tag{28}$$

where μ is Earth's gravitational parameter. The algorithm is forced to evaluate at the specified final time. For the unperturbed case an orbit closure check is performed, i.e. the final state is compared with the initial state as a measure of accuracy:

$$||\epsilon_{\mathbf{r}}|| = \frac{||\mathbf{r}(t_f) - \mathbf{r}(t=0)||}{\|\mathbf{r}(t=0)\|} \tag{29}$$

$$||\epsilon_{\mathbf{v}}|| = \frac{||\mathbf{v}(t_f) - \mathbf{v}(t=0)||}{\|\mathbf{v}(t=0)\|} \tag{30}$$

Additionally, the conservation of total energy generally given by Eq. (31) for up to the J_2 zonal perturbation is used as another accuracy check as shown in Eq. (32)

$$E(t) = \frac{1}{2}v(t)^2 - \frac{\mu}{r(t)} \underbrace{- \frac{J_2}{2}\frac{\mu}{r(t)}\left(\frac{r_{eq}}{r(t)}\right)^2 \left(3\left(\frac{z(t)}{r(t)}\right)^2 - 1\right)}_{\text{Only when } J_2 \text{ is considered}} \underbrace{+ \cdots}_{\text{H.O.T.}} \tag{31}$$

$$\epsilon_E(t) = \left|\frac{E(t) - E(t_0)}{E(t_0)}\right| \tag{32}$$

Combining those two measures of accuracy produces confidence in the results shown below. The results in the following subsections were obtained using $tol = 10^{-15}$ and $n = 28$ for the variable time step in Eq. (15), and an initial study on the combined effect of the order, n, of the analytical continuation series expansion and tol is discussed later.

The Geostationary Orbit (GEO)

For the unperturbed case the simulation results generated by *AC* the algorithm uses 5 time-steps to compute 1 orbit to machine precision as shown in Figure 2 for the conservation of total energy check.

For the J_2 perturbation, to maintain accuracy Equation 15 adapts the time step size in such a manner that the number of steps is increased from 5, in the unperturbed case, to 6 for J_2 perturbation. Figure 3 shows the energy check results obtained from the *AC* algorithm.

Also, it is found that $||\epsilon_{\mathbf{r}}|| = 1.62616 \times 10^{-15}$ and $||\epsilon_{\mathbf{v}}|| = 6.28066 \times 10^{-16}$.

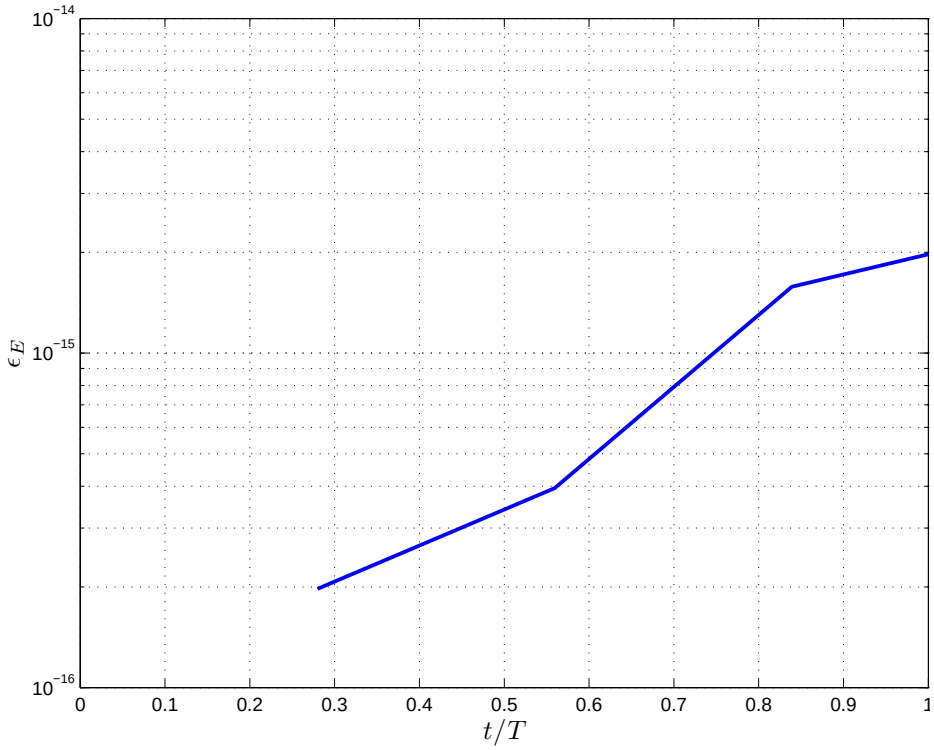

Figure 2. Energy conservation check, unperturbed GEO.

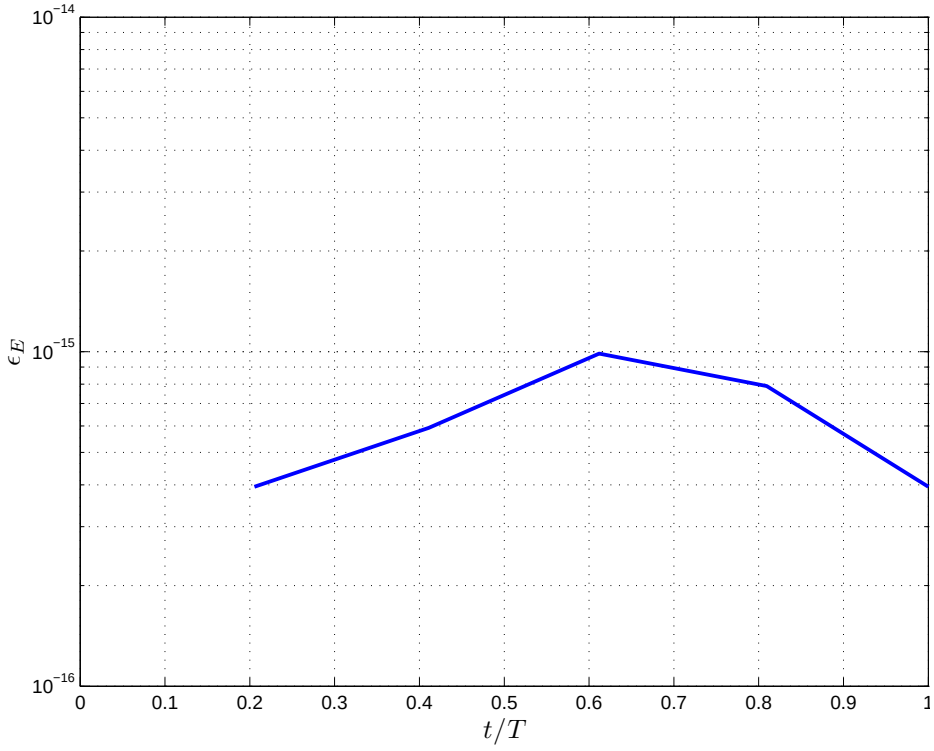

Figure 3. Energy conservation check, J_2 GEO.

The Low Earth Orbit (LEO)

For the unperturbed case the simulation results generated by *AC* the algorithm uses 15 time-steps to compute 1 orbit to machine precision as shown in Figure 4 for the conservation of total energy check.

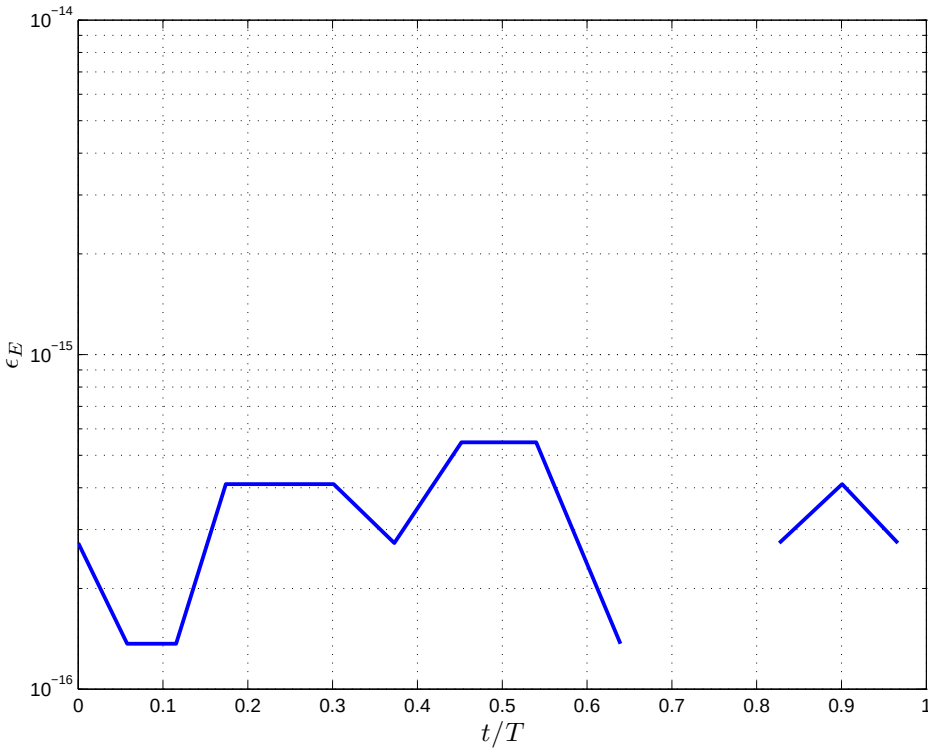

Figure 4. Energy conservation check, unperturbed LEO.

For the J_2 perturbation, to maintain accuracy Eq. (15) uses the same number of time steps, but it adapts when it is evaluated for J_2 perturbation in order to maintain accuracy. Figure 5 shows the energy check results obtained from the *AC* algorithm.

For this case, the orbit closure check resulted in near machine precision: $||\epsilon_{\mathbf{r}}|| = 4.69565 \times 10^{-16}$ and $||\epsilon_{\mathbf{v}}|| = 6.36947 \times 10^{-16}$.

Of course, these very high precision closures are used to demonstrate the robustness of the numerical method. We all understand that the physical precision of the J_2-only perturbation is much less. It is easy to relax the target tolerance and reduce the order of expansion as presented in (15) in order to obtain closure errors consistent with the physical precision of a given force model.

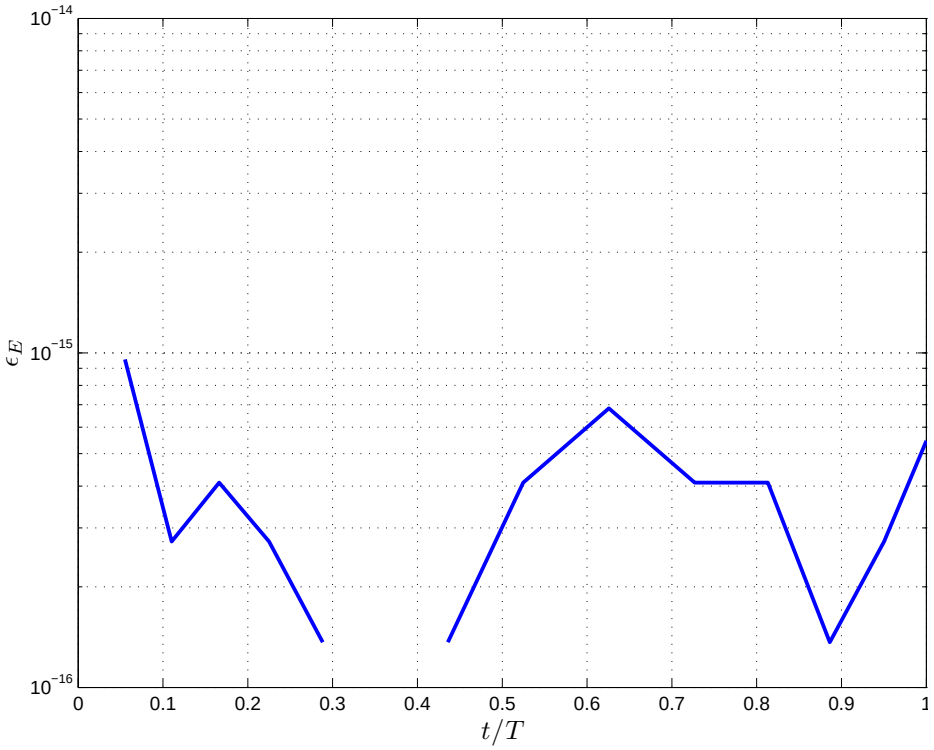

Figure 5. Energy conservation check, J_2 LEO.

The Highly Eccentric Orbit (HEO)

For the unperturbed case, the simulation results generated by *AC* are shown in Figure 6 for the conservation of total energy check. With 55 steps taken, energy is conserved to very high accuracy as shown in Figure 6

For the J_2 perturbation the algorithm uses 65 steps instead of 55 as in the unperturbed case. This results in a better accuracy than the former case, but still not machine precision. Figure 7 shows the energy check results obtained from the *AC* algorithm.

For this case, the orbit closure check resulted in $||\epsilon_{\mathbf{r}}|| = 1.47971 \times 10^{-12}$ and $||\epsilon_{\mathbf{v}}|| = 7.7887 \times 10^{-13}$. Clearly these closure errors remain very small compared to the physical accuracy of this model, and in fact "state of the art" force models cannot predict orbit closure to better than $||\epsilon_{\mathbf{r}}|| \approx 10^{-7}$. In the next subsection we study the accuracy of the algorithm for different parameters to understand this accuracy loss.

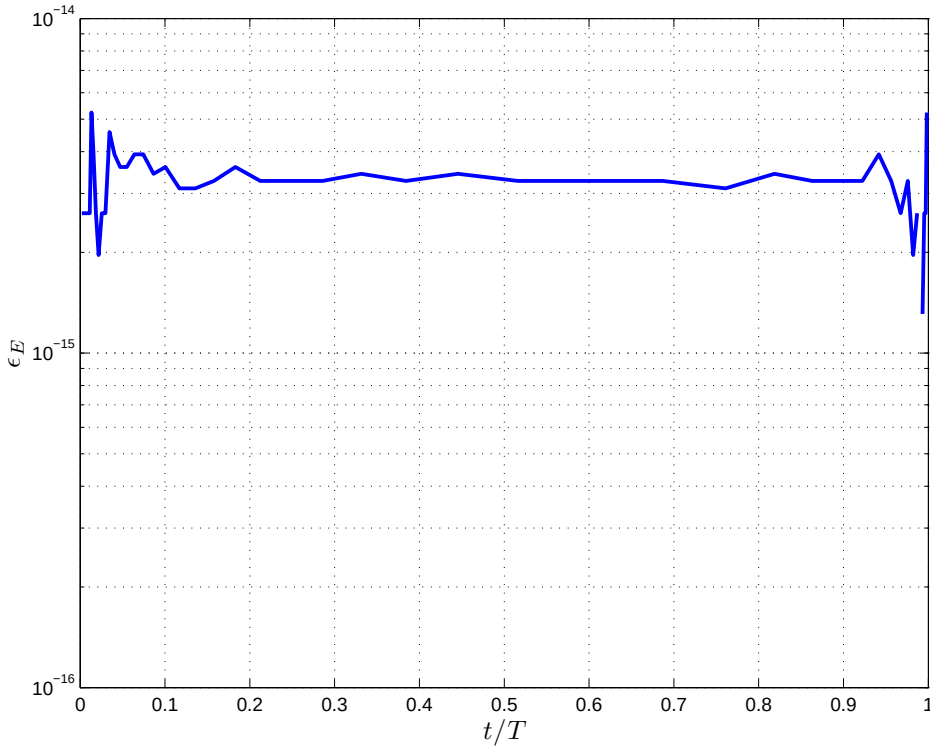

Figure 6. Energy conservation check, unperturbed HEO.

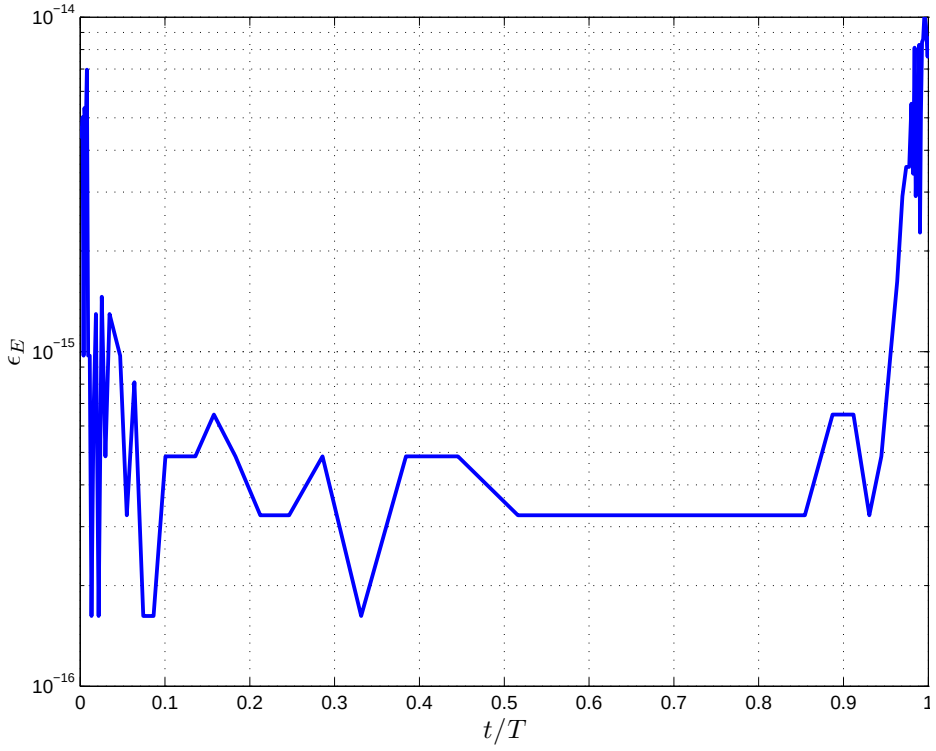

Figure 7. Energy conservation check, J_2 HEO.

Combined effect of n and tol

In order to study the combined effect of n and tol in (15), the J_2 case was studied for the HEO introduced above. The measure chosen to describe the accuracy of the method for a particular set of parameter values is the sum of the squares of the residuals of energy normalized by the initial energy:

$$||\epsilon_E|| = \left(\sum_{i=1}^{n\text{steps}} \epsilon_E^2(t_i) \right)^{1/2} \tag{33}$$

where t_i correspond to the i^{th} instant at which a solution was calculated. Figures 8 and 9 show the results obtained varying the target tolerance values, tol, using double and quadruple precision computations, respectively. The inclusion of quadruple precision computations addresses the effects of round-off errors (those resulting from finite memory for storing numbers and performing computations) and provides a better way to assess the effect of the tuning parameters on the *AC* achieved accuracy. For easier comparison, corresponding plots have the same scales regardless of the particular area covered by the curves plotted. The effects of varying the order of expansion, n, is shown in figures 10 and 11 for double and quadruple precision, respectively.

Comparing the double precision results with their quadruple precision counterparts suggest that, even though reducing the value of tol in Eq. (15) reduces the accuracy of the algorithm for a fixed expansion order n, this effect is bounded by the machine precision. When close to double precision's limit, round-off errors become more important and reducing tol at that point have unpredictable effects. For instance, the accuracy obtained for the example case studied using $n = 15$ and $tol = 10^{-15}$ underperformed compared to the results obtained with $tol = 10^{-10}$–10^{-14} when using double precision, but expected behavior results from using quadruple precision to perform computations using the same parameters.

The effect of the expansion order, n, is not trivial. Equation 15 shows factors may compete as n is increased. Although the factor $(n!)^{(1/n)}$ increases with n, the same cannot be guaranteed for the factor $(1/||\mathbf{r}^{(n)}||)^{(1/n)}$ and their rates may vary relative to one another. Figure 11 shows that initially the accuracy for the case studied can be enhanced by incrementing n but, after a sweet spot that seems to depend on the value of tol, this relation is reversed suggesting the n^{th} derivative factor starts increasing with n slower than the factorial part, resulting in larger step sizes that reduce the overall performance.

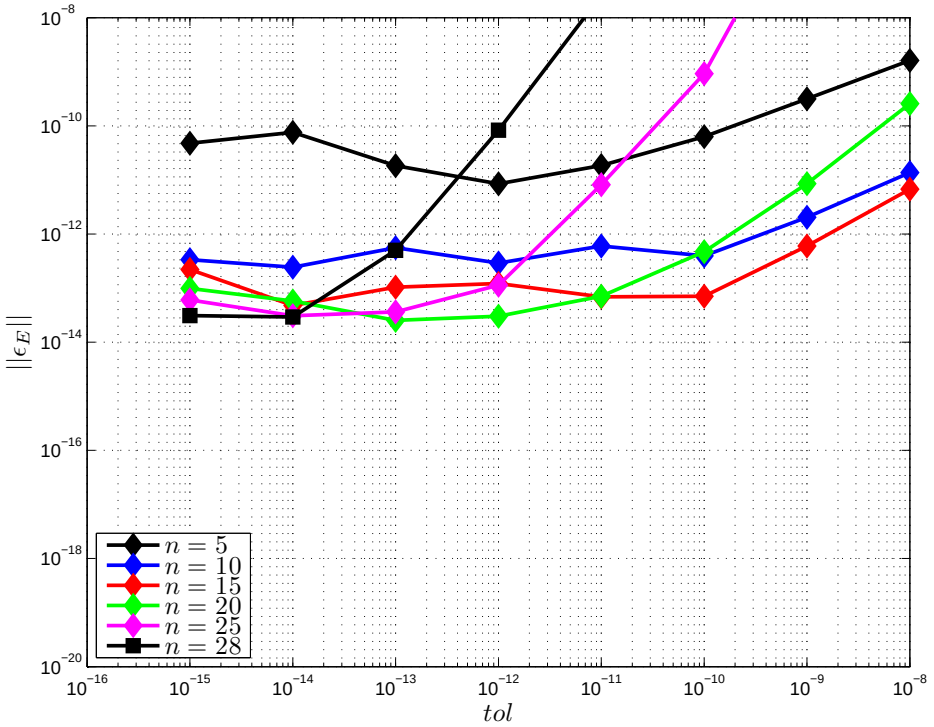

Figure 8. Effect of tol on $||\epsilon_E||$ for different values of n. Results computed using double precision. J_2 case for HEO.

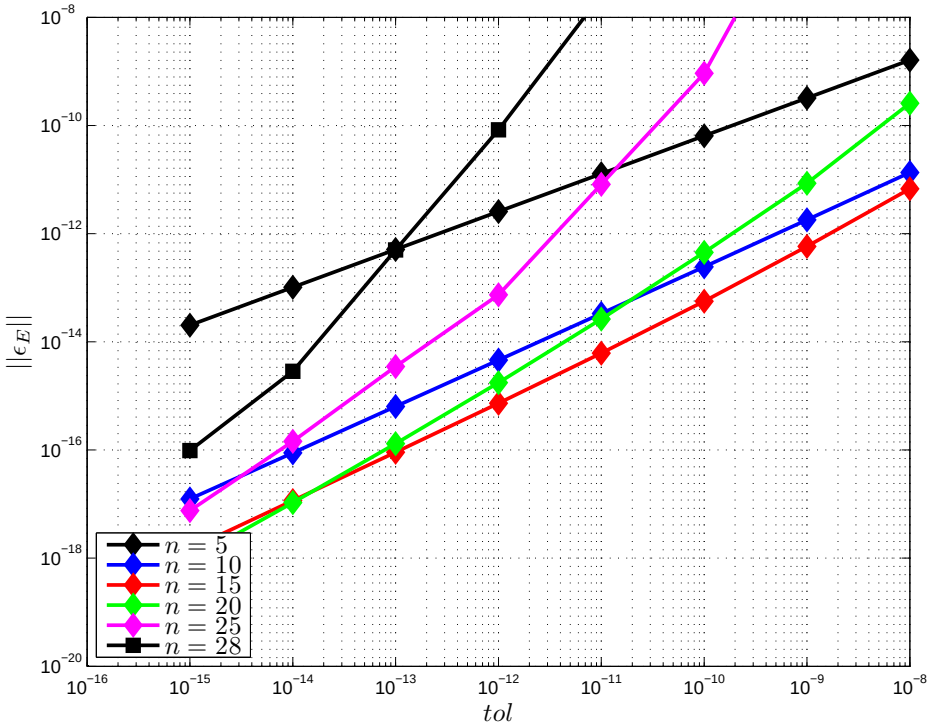

Figure 9. Effect of tol on $||\epsilon_E||$ for different values of n. Results computed using quadruple precision. J_2 case for HEO.

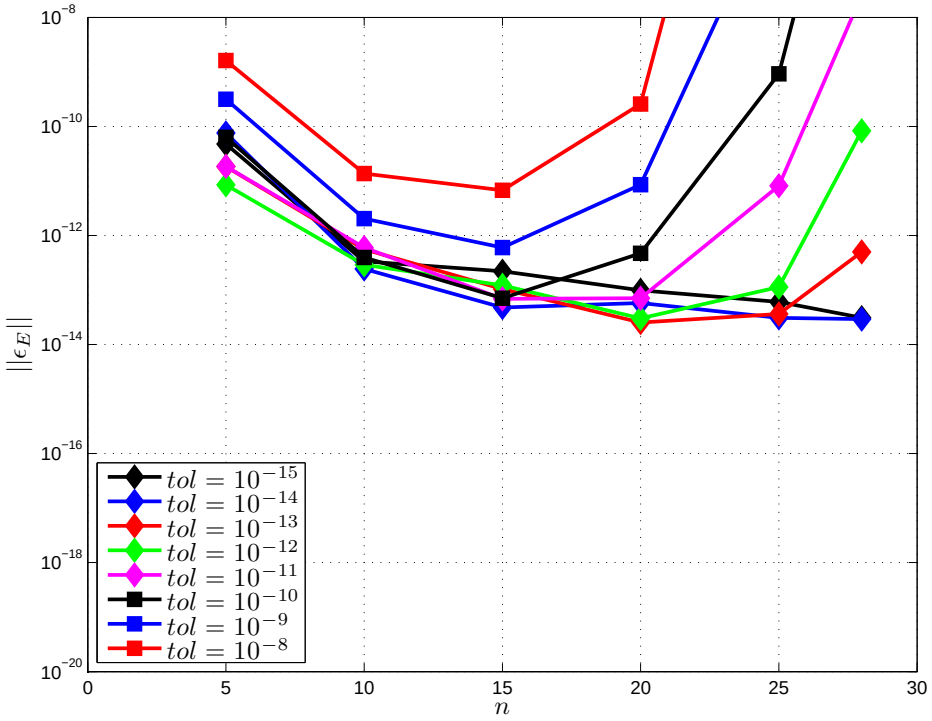

Figure 10. Effect of n on $||\epsilon_E||$ for different values of tol. Results computed using double precision. J_2 case for HEO.

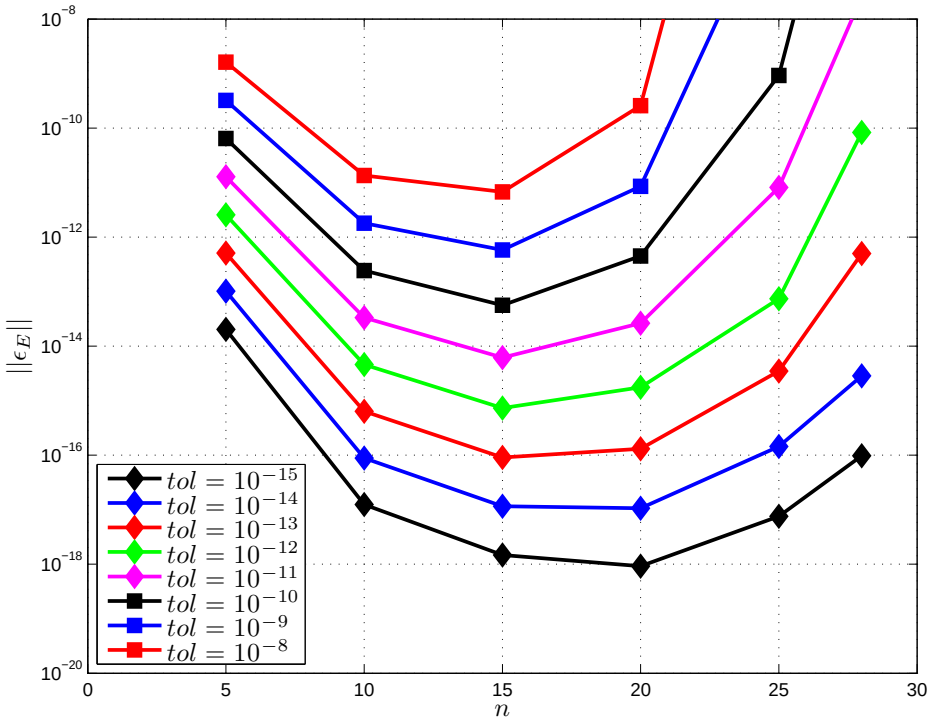

Figure 11. Effect of n on $||\epsilon_E||$ for different values of tol. Results computed using quadruple precision. J_2 case for HEO.

CONCLUSION

The algorithm presented in this paper computes arbitrary time derivatives of the perturbed two-body problem using a recursive formulation. Energy conservation and orbit closure (for the unperturbed case) are used to measure algorithm accuracy, obtaining close-to-machine precision accuracy. Effect of algorithm parameters on the accuracy of the solutions is examined and preliminary results suggest that machine precision can be achieved but round-off errors start playing an important role. Even though the adaptive time step size equation used improves largely over previous results, its dependency on the expansion order is nontrivial; this relation will be studied further in the future.

The J_2 term solution is enhanced to yield substantially more accurate results than previous studies. The present study provides a solution that is accurate but requires a small fraction of the sample points compared with common integrators. This work is currently being expanded to include J_3–J_6 terms and the State Transition Matrix, where the methodology is presented in this paper. Both the series trajectory and state transition matrix solutions are expected to be broadly useful for applications not requiring high-order gravity perturbation models.

REFERENCES

[1] R. Battin, *An introduction to the mathematics and methods of astrodynamics*. AIAA, 1987.

[2] H. Schaub and J. Junkins, *Analytical mechanics of space systems*. AIAA, 2003.

[3] E. Fehlberg, "Low-order classical Runge-Kutta formulas with stepsize control and their application to some heat transfer problems," tech. rep., NASA, 1969.

[4] S. Filippi and J. Gräf, "New Runge–Kutta–Nyström formula-pairs of order 8 (7), 9 (8), 10 (9) and 11 (10) for differential equations of the form $y" = f(x, y)$," *Journal of computational and applied mathematics*, Vol. 14, No. 3, 1986, pp. 361–370.

[5] K. Fox, "Numerical integration of the equations of motion of celestial mechanics," *Celestial mechanics*, Vol. 33, No. 2, 1984, pp. 127–142.

[6] J. Jackson, "Note on the numerical integration of $d^2x/dt^2 = f(x, t)$," *Monthly Notices of the Royal Astronomical Society*, Vol. 84, 1924, pp. 602–606.

[7] M. M. Berry and L. M. Healy, "Implementation of Gauss-Jackson integration for orbit propagation," *The Journal of the Astronautical Sciences*, Vol. 52, No. 3, 2004, pp. 331–357.

[8] J. Dormand, M. El-Mikkawy, and P. Prince, "High-order embedded Runge-Kutta-Nystrom formulae," *IMA Journal of Numerical Analysis*, Vol. 7, No. 4, 1987, pp. 423–430.

[9] O. Montenbruck, "Numerical integration methods for orbital motion," *Celestial Mechanics and Dynamical Astronomy*, Vol. 53, No. 1, 1992, pp. 59–69.

[10] K. Hadjifotinou and M. Gousidou-Koutita, "Comparison of numerical methods for the integration of natural satellite systems," *Celestial Mechanics and Dynamical Astronomy*, Vol. 70, No. 2, 1998, pp. 99–113.

[11] P. W. Sharp, "N-body simulations: The performance of some integrators," *ACM Transactions on Mathematical Software (TOMS)*, Vol. 32, No. 3, 2006, pp. 375–395.

[12] X. Bai and J. L. Junkins, "Modified Chebyshev-Picard Iteration Methods for Orbit Propagation," *The Journal of the Astronautical Sciences*, Vol. 58, No. 4, 2011, pp. 583–613.

[13] X. Bai and J. L. Junkins, "Modified Chebyshev-Picard iteration methods for solution of initial value problems," *The Journal of the Astronautical Sciences*, Vol. 59, No. 1-2, 2012, pp. 335–359.

[14] J. Junkins, A. Bani Younes, R. Woollands, and X. Bai, "Orthogonal Approximation in Higher Dimensions: Applications in Astrodynamics," *ASS 12-634, JN Juang Astrodynamics Symp*, 2012.

[15] B. Macomber, R. Woollands, A. Probe, A. Younes, X. Bai, and J. Junkins, "Modified Chebyshev Picard Iteration for Efficient Numerical Integration of ordinary Differential Equations," *Advanced Maui Optical and Space Surveillance Technologies Conference*, Vol. 1, 2013, p. 89.

[16] A. Probe, B. Macomber, D. Kim, R. Woollands, and J. L. Junkins, "Terminal Convergence Approximation Modified Chebyshev Picard Iteration for efficient numerical integration of orbital trajectories," *Advanced Maui Optical and Space Surveillance Technologies Conference,, Maui, Hawaii*, 2014.

[17] A. B. Probe, B. Macomber, J. I. Read, R. M. Woollands, and J. L. Junkins, "RADIALLY ADAPTIVE EVALUATION OF THE SPHERICAL HARMONIC GRAVITY SERIES FOR NUMERICAL ORBITAL PROPAGATION," *AAS/AIAA Space Flight Mechanics Meeting, Williamsburg, VA*, 2015.

[18] B. Macomber, A. Probe, R. Woollands, and J. L. Junkins, "Automated Tuning Parameter Selection for Orbit Propagation with Modified Chebyshev Picard Iteration," *AAS/AIAA Spaceflight Mechanics Meeting, Williamsburg, VA*, 2015.

[19] R. Woollands, A. Younes, B. Macomber, A. Probe, D. Kim, and J. Junkins, "Validation of Accuracy and Efficiency of Long-Arc Orbit Propagation Using the Method of Manufactured Solutions and the Round-Trip-Closure Method," *Advanced Maui Optical and Space Surveillance Technologies Conference*, Vol. 1, 2014, p. 19.

[20] R. Woollands and J. Junkins, "A New Solution for the General Lamberts Problem," *37th Annual AAS Guidance & Control Conference, Breckenridge, CO*, 2014.

[21] R. M. Woollands, J. L. Read, B. Macomber, A. Probe, A. B. Younes, and J. L. Junkins, "METHOD OF PARTICULAR SOLUTIONS AND KUSTAANHEIMO-STIEFEL REGULARIZED PICARD ITERATION FOR SOLVING TWO-POINT BOUNDARY VALUE PROBLEMS," *AAS/AIAA Spce Flight Meeting, Williamsburg, VA*, 2015.

[22] R. Woollands, A. Bani-Younes, B. Macomber, X. Bai, and J. Junkins, "A New Solution for the General Lamberts Problem," *38th Annual AAS Guidance & Control Conference, Breckenridge, CO*, 2014.

[23] J. M. Aristoff and A. B. Poore, "Implicit Runge–Kutta methods for orbit propagation," *Proceedings of the 2012 AIAA/AAS Astrodynamics Specialist Conference*, Vol. 4880, 2012, pp. 1–19.

[24] B. K. Bradley, B. A. Jones, G. Beylkin, and P. Axelrad, "A new numerical integration technique in astrodynamics," *22nd AAS/AIAA Space Flight Mechanics Meeting, Charleston, SC*, 2012, pp. 12–216.

[25] B. K. Bradley, B. A. Jones, G. Beylkin, K. Sandberg, and P. Axelrad, "Bandlimited implicit Runge–Kutta integration for astrodynamics," *Celestial Mechanics and Dynamical Astronomy*, Vol. 119, No. 2, 2014, pp. 143–168.

[26] T. A. Elgohary, L. Dong, J. L. Junkins, and S. N. Atluri, "A Simple, Fast, and Accurate Time-Integrator for Strongly Nonlinear Dynamical Systems," *CMES: Computer Modeling in Engineering & Sciences*, Vol. 100, No. 3, 2014, pp. 249–275.

[27] T. A. Elgohary, L. Dong, J. L. Junkins, and S. N. Atluri, "Time Domain Inverse Problems in Nonlinear Systems Using Collocation & Radial Basis Functions," *CMES: Computer Modeling in Engineering & Sciences*, Vol. 100, No. 1, 2014, pp. 59–84.

[28] T. A. Elgohary, J. L. Junkins, and S. N. Atluri, "AN RBF-COLLOCATION ALGORITHM FOR ORBIT PROPAGATION," *Advances in Astronautical Sciences: AAS/AIAA Space Flight Mechanics Meeting*, 2015.

[29] J. D. Turner, T. A. Elgohary, M. Majji, and J. L. Junkins, "High accuracy trajectory and uncertainty propagation algorithm for long-term asteroid motion prediction," *Adventures on the Interface of Mechanics and Control* (K. Alfriend, M. Akella, J. Hurtado, and J. Turner, eds.), pp. 15–34, Tech Science Press, 2012.

[30] T. A. Elgohary and J. D. Turner, "State Transition Tensor Models for the Uncertainty Propagation of the Two-Body Problem," *Advances in Astronautical Sciences: AAS/AIAA Astrodynamics Conference*, Vol. 150, 2014, pp. 1171–1194.

[31] T. A. Elgohary, J. D. Turner, and J. L. Junkins, "High-Order Analytic Continuation and Numerical Stability Analysis for the Classical Two-Body Problem," *Advances in Astronautical Sciences: The Jer-Nan Juang Astrodynamics Symposium*, Vol. 147, 2012, pp. 627–646.

[32] T. A. Elgohary, D. Kim, J. D. Turner, and J. L. Junkins, "An Efficient Algorithm for Perturbed Orbit Integration Combining Analytical Continuation and Modified Chebyshev Picard Iteration," *Advanced Maui Optical and Space Surveillance Technologies Conference*, Vol. 1, 2014, p. 18.

[33] J. D. Turner and T. A. Elgohary, "Analytic Orbit Trajectory Prediction for J2-J6 Using Recursive Lagrange-Like Invariants," *Advanced Maui Optical and Space Surveillance Technologies Conference*, Vol. 1, 2013, p. 108.

[34] D. Kim and J. D. Turner, "Variable Step-Size Control for Analytic Power Series Solutions for Orbit Propagation," *Proceedings of the AIAA/AAS Astrodynamics Specialist Conference, San Diego, CA*, AIAA, 2014.

[35] J. Read, B. Macomber, A. B. Younes, J. Turner, and J. Junkins, "Efficient Orbit Propagation of Orbital Elements Using Modified Chebyshev Picard Iteration Method," Submitted to Journal of Astronautical Sciences August 2015, 2015.